Desalination and Water Treatment
www.deswater.com

doi: 10.5004/dwt.2018.21869

102 (2018) 220–228
January

High efficiency removal of Pb(II) by modified spent compost of *Hypsizygus marmoreus* in a fixed-bed column

Yunlong Yang[a,b], Ershu Lin[a], Xin Tao[a], Kaihui Hu[a,b,*]

[a]*College of Life Science, Fujian Agriculture and Forestry University, Fuzhou, Fujian, China, emails: 474585312@qq.com (K. Hu), longyunyang@126.com (Y. Yang), 564448951@qq.com (E. Lin), 1316284816@qq.com (X. Tao)*
[b]*Institute of Mushroom Industry, Fujian Agriculture and Forestry University, Gutian, Fujian, China*

Received 24 August 2017; Accepted 30 December 2017

ABSTRACT

The spent compost of *Hypsizygus marmoreus* (SCHM) modified by NaOH solution was used as a novel biosorbent (MSCHM) to remove Pb(II) ions from aqueous solution in this study. Batch adsorption experiments revealed that the uptake capacity increased from 54.8 mg/g by SCHM to 72.5 mg/g by MSCHM and the adsorption efficiency improved regardless of the initial Pb(II) concentration. In the fixed-bed column experiments, the breakthrough and exhaustion time were extended/shorten about 2–11 times with the flow rate, bed depth and initial concentration changing from 20 mL/min, 12 cm and 45 mg/L to 40 mL/min, 28 cm and 145 mg/L, respectively. The adsorption process was predicted and described well by Thomas model indicating the external and internal diffusions were not the bottleneck of the process. The regeneration experiments were conducted to validate the reuse effectiveness of MSCHM, and the final regeneration efficiency achieved to 73%. Furthermore, the preliminary adsorption mechanisms of Pb(II) onto MSCHM were investigated by Brunauer–Emmett–Teller method, scanning electron microscope and Fourier transform infrared (FT-IR) spectrometer, and carboxyl, hydroxyl and amide might be important functional groups adsorbing Pb(II) ions.

Keywords: Spent compost of *Hypsizygus marmoreus*; Biosorption; Pb(II) removal; Fixed-bed column

1. Introduction

The rapid increase of industrialization has led to excessive releasing of toxic metal ions such as lead, cadmium, mercury, chromium, arsenic and copper into the environment, and they are not naturally degraded. Among these metal ions, Pb(II) is highly toxic in nature. It is not only an environmental oncogenic metal that induces immunotoxicity and anemia but also in close relation with endoplasmic reticulum–driven apoptosis and autophagy [1]. Long-term exposure to trace levels of Pb may play a role in the development of coronary atherosclerotic plaques [2]. Unfortunately, more and more industrial products or wastes including metal plating, oil refining, battery manufacturing, fossil fuels, paints, ceramics, plumbing materials, glass, printing and photographic materials, contribute to the entry of Pb into the environment in recent years [3,4].

Accordingly, it is necessary to develop a cost-effective and efficient way to retrieve lead from contaminated environments especially from water. As a matter of fact, a variation of techniques such as biological contactor reactor [5], chelating agent [6], complexation–microfiltration [7], membrane separation [8], ion exchange [9], constructed wetlands [10] and adsorption have been used to remove Pb(II) from wastewater. Out of them, adsorption is regarded as the most effective method for Pb(II) removal due to its easy handling, low cost and easily available adsorbents [11], and thus natural inorganic materials were used widely to remove Pb(II) from aqueous solutions (phosphate rocks, alumina, activated alumina, silica gel, zeolite, clays, activated carbon, soil, river sediment and others) [12]. Also, a synthetic polymer was

* Corresponding author.

reported to be an attractive adsorbent for removing toxic metal ions from aqueous solution [13]. Nevertheless, attention has been increasingly paid to agriculture and food industry wastes since these wastes usually have a good capacity to bind heavy metals.

As the largest producer of the edible fungi, China generates a huge number of spent mushroom compost (SMC) every year, which has put a lot of pressure on the local environment. SMC comprises abundant functional groups including hydroxyl, carbonyl, carboxyl, amino and phosphate, all of which are capable of chelating heavy metal ions in aqueous solution. Based on this point, various SMCs were utilized to adsorb metals: biosorption of Mn(II) ions by *Pleurotus* SMC [14], biosorption of Zn^{2+} by spent substrates of *Pleurotus ostreatus* [15], biosorption of Cu^{2+} by spent substrate of fragrant mushroom [16], removal of Cr(VI) by *Auricularia auricula* spent substrate [17] and biosorption of lead(II) by spent mushroom *Tricholoma lobayense* [18]. To our knowledge, however, no research on heavy metal ions adsorption by spent compost of *Hypsizygus marmoreus* (SCHM) has been reported so far. Furthermore, in order to improve adsorption capacity, SMCs have to be subjected to grinding and immobilization, which could bring about cost increase and secondary pollution from the view of engineering application.

The aim of the present study is to assess the efficiency of lead(II) adsorption by modified spent compost of *Hypsizygus marmoreus* (MSCHM). In batch adsorption experiments, the uptake capacity of SCHM and MSCHM was analyzed. In a fixed-bed column, the effect of bed height, influent concentration and flow rate on the breakthrough and exhaustion time were explored. For the preliminary adsorption mechanism of Pb(II), Brunauer–Emmett–Teller (BET), scanning electron microscope (SEM) and Fourier transform infrared (FT-IR) techniques were employed. Besides, regeneration experiments were conducted to determine regeneration parameters.

2. Experimental setup

2.1. Pretreatment and modification of SCHM

SCHM was obtained from Gutian, Fujian, China. After grinding by hand, SCHM was dried in air for 1 d. 200 g of dried SCHM was put into 1 L of purified water, and shaken with a rotation speed of 100 rpm at room temperature for 4 h to release organic matters contained in SCHM. Subsequently, the mixture was settled for 30 min, and then the supernatant including particles with a small density was decanted to obtain the materials with a good settling ability. The resultant SCHM was washed with purified water several times until flushing water was grossly clear. Following drying in an oven at 60°C overnight, SCHM was stored in an air-tight container for further use.

For modification, 20 g of SCHM processed above was mixed with 0.8 L of NaOH solution (4%) and oscillated with a rotation speed of 200 rpm at room temperature for 3 h. After 30 min of settlement, SCHM was separated from the supernatant and washed with purified water until pH of SCHM approached 7. The modified SCHM (MSCHM) was dried in an oven at 60°C overnight, and immediately stored in an air-tight container.

2.2. Preliminary adsorption mechanisms for biosorbent

In order to explore preliminary adsorption mechanisms, SEM, BET and FT-IR were preformed on both SCHM and MSCHM samples. For surface morphology, SCHM and MSCHM were fixed with glutaraldehyde and analyzed using a SEM (Inspect F50, FEI, USA). Surface area, pore volume and pore diameter were measured according to a previous report [19]. FT-IR was carried out with KBr pellet technique. In brief, the biosorbent was pressed into pellet with a mass ratio of sample to KBr being 1:100. Afterwards the pellet was scanned through a FT-IR spectrometer (Nicolet iS10, Thermo Fisher, USA) in a frequency range of 4,000–400 cm^{-1} to gain FT-IR spectral data, following which the possible functional groups were determined.

2.3. Batch experiments for biosorption

Batch experiments were performed in 250-mL flasks containing 100 mL artificial wastewater and 0.1 g biosorbent at room temperature with a rotation speed of 150 rpm and pH value of 6. All the adsorption experiments were conducted in triplicate. The adsorption efficiency (AE) at a certain time and adsorption capacity of biosorbents (q_b) at equilibrium were determined with the following equations:

$$AE = \frac{C_i - C_c}{C_i} \times 100\% \tag{1}$$

$$q_b = \frac{(C_i - C_e)V}{m} \tag{2}$$

where C_i, C_c and C_e represent the Pb(II) concentration (mg/L) at the start, a certain time and equilibrium, respectively, while V is the solution volume and m is indicative of the mass of biosorbent.

2.4. Fixed-bed column experiments for biosorption

For the adsorption of Pb(II) in a fixed-bed column, a down-flow plexiglass column with an internal diameter of 2 cm and length of 50 cm was used. To investigate the effect of bed depth on adsorption, the column was packed with 6, 10 and 14 g MSCHM, which corresponded to 12, 20 and 28 cm, respectively. Various concentrations of 45, 90 and 140 mg/L and flow rates of 20, 30 and 40 mL/min were selected to investigate the effect of initial Pb(II) concentration and flow rate on adsorption, respectively.

In order to evaluate the breakthrough curves, the breakthrough time and exhaustion time were adopted. The breakthrough time was the point where the effluent concentration (C_t) from the column was approximately 5% of the influent concentration (C_0), while the exhaustion time was regarded as the point where the effluent concentration accounted for 90% of the influent concentration. Additionally, the following equation was used to determine the total mass of adsorbed metal represented by the area under the breakthrough curve at a given feeding concentration and flow rate:

$$M_{\mathrm{Pb}} = \frac{Q}{1000}\int_0^{\mathrm{total}} C_{\mathrm{cad}}\,\mathrm{d}t = \frac{Q}{1000}\int_0^{\mathrm{total}} (C_0 - C_t)\,\mathrm{d}t \tag{3}$$

where M_{Pb}, Q, C_0 and C_t are the total mass of adsorbed Pb (mg), flow rate through the column (mL/min), influent and effluent concentration (mg/L), respectively.

The uptake capacity (q_e, mg/g), namely the amount of Pb(II) adsorbed per gram of MSCHM at equilibrium, can be calculated according to the following equation:

$$q_e = \frac{M_{Pb}}{m} \tag{4}$$

2.5. Breakthrough curves modeling

Some mathematical models such as Adams–Bohart and Thomas models were established to predict the breakthrough curve for the metallic solution, and they play an important role in designing and optimizing the fixed-bed column adsorption process. In the current study, Thomas model was used to match the experimental data to predict the dynamic adsorption behavior of Pb(II) onto the biosorbent of MSCHM loaded in a fixed-bed column.

2.6. Regeneration experiments

To evaluate the stability of the modified biosorbents, the regeneration experiments were carried out after MSCHM was exhausted because of Pb(II) adsorption. The adsorbent of MSCHM was first eluted in the down-flow direction at a flow rate of 30 mL/min with 0.1 M HCl for about 120 min. Then, the distilled water was used to wash the column till to pH value of 5.0–6.0, after which the column was reused for the next cycle of adsorption. The process of adsorption–desorption continued three times in succession and the regeneration efficiency (RE) was calculated as following:

$$RE = \frac{\text{mass of Pb(II) desorbed}}{\text{mass of Pb(II) adsorbed}} \times 100\% \tag{5}$$

2.7. Chemicals, reagents and Pb(II) measurement

All chemicals used in this study are analytical grade. As the stock solution, 1 g/L of Pb(II), was prepared by dissolving appropriate amount of plumbous nitrate into deionized water, which could be further diluted to prepare the working solution at desired concentration. All the pHs for solution were adjusted by 0.1 M NaOH or 0.1 M HCl. Pb(II) was measured by xylenol orange spectrophotometric method [20].

3. Results

3.1. Characteristics of SCHM and MSCHM

The characteristics of SCHM and MSCHM in dry status and in water are displayed in Fig. 1. Clearly, the modified biosorbent (Fig. 1(b)) was a little darker than the raw biosorbent (Fig. 1(a)). After the pretreatment process during which the particles with small density were completely removed, the left mainly composed of wood chips and cottonseed hull almost in the same proportion had advantages in appropriate size, rigidity. Fig. 1(c) shows a clear interface of liquid–solid for MSCHM, and the density was calculated to be about 1.2 g/mL.

3.2. Batch adsorption experiments

Fig. 2 shows the results of batch adsorption experiments including the changing trend of Pb(II) adsorbed by SCHM and MSCHM and AE at 30 min with different initial concentration. Pb(II) decreased from 84 to 29.2 mg/L and 11.5 mg/L when SCHM and MSCHM were used as biosorbents with the sorption capacity being 54.8 and 72.5 mg/g, respectively, and it took almost 120 min to reach the equilibrium point of adsorption (Fig. 2(a)). Also, it can be seen from Fig. 2(b) that no matter what the initial concentration is, AE was enhanced. For example, the AE at 30 min was 43.9% for SCHM and 60.6% for MSCHM at Pb(II) concentration of 66 mg/L. In addition, the biosorption capacity of MSCHM was compared with that of other composts and results were outlined in Table 1.

3.3. Adsorption experiments in a fixed-bed column

3.3.1. Effect of flow rate

The biosorption breakthrough curves of MSCHM obtained with different flow rate are displayed in Fig. 3(a). Clearly, much steeper breakthrough curves and shorter breakthrough time were observed at relatively higher flow rates. The breakthrough time was 249, 163 and 75 min, and the exhaustion time was 859, 515 and 421 min when the flow rate was 20, 30 and 40 mL/min, respectively. Similarly, the adsorption capacity dropped from 97.7 to 87.3 mg/g with the flow rate climbing from 20 to 40 mL/min.

3.3.2. Effect of bed depth

The bed depth is a critical parameter for the evaluation of biosorbent performance, which can be seen from Fig. 3(b) where the effect of bed depth on the shape of breakthrough curves was displayed. The increase of bed height not only improved the adsorption capacity but also prolonged obviously both breakthrough and exhaustion time. When the bed depth was 12, 20 and 28 cm with the corresponding MSCHM being 6, 10 and 14 g, the uptake capacity was 83.2, 87.7 and 98.7 mg/g, respectively. The breakthrough time extended from 25 min at 12 cm to 316 min at 28 cm, while the exhaustion time prolonged from 332 min at 12 cm to 657 min at 28 cm.

3.3.3. Effect of initial Pb(II) concentration

The metal ion concentration is also regarded as an important parameter in a fixed-bed column. Fig. 3(c) exhibits the effect of different Pb(II) concentrations on the adsorption process. The breakthrough time was shortened from 344 to 110 min, and the exhaustion time was cut from 880 to 333 min, as the influent concentration of Pb(II) elevated from 50 to 140 mg/L. For the uptake capacity, the opposite trend, however, was observed that it increased from 83.6 to 94.8 mg/g with Pb(II) concentration increasing from 50 to 140 mg/L.

3.4. Breakthrough curves modeling

To predict the maximum adsorption capacity of MSCHM in the current fixed-bed column, Thomas model was used, the equation of which was described as follows:

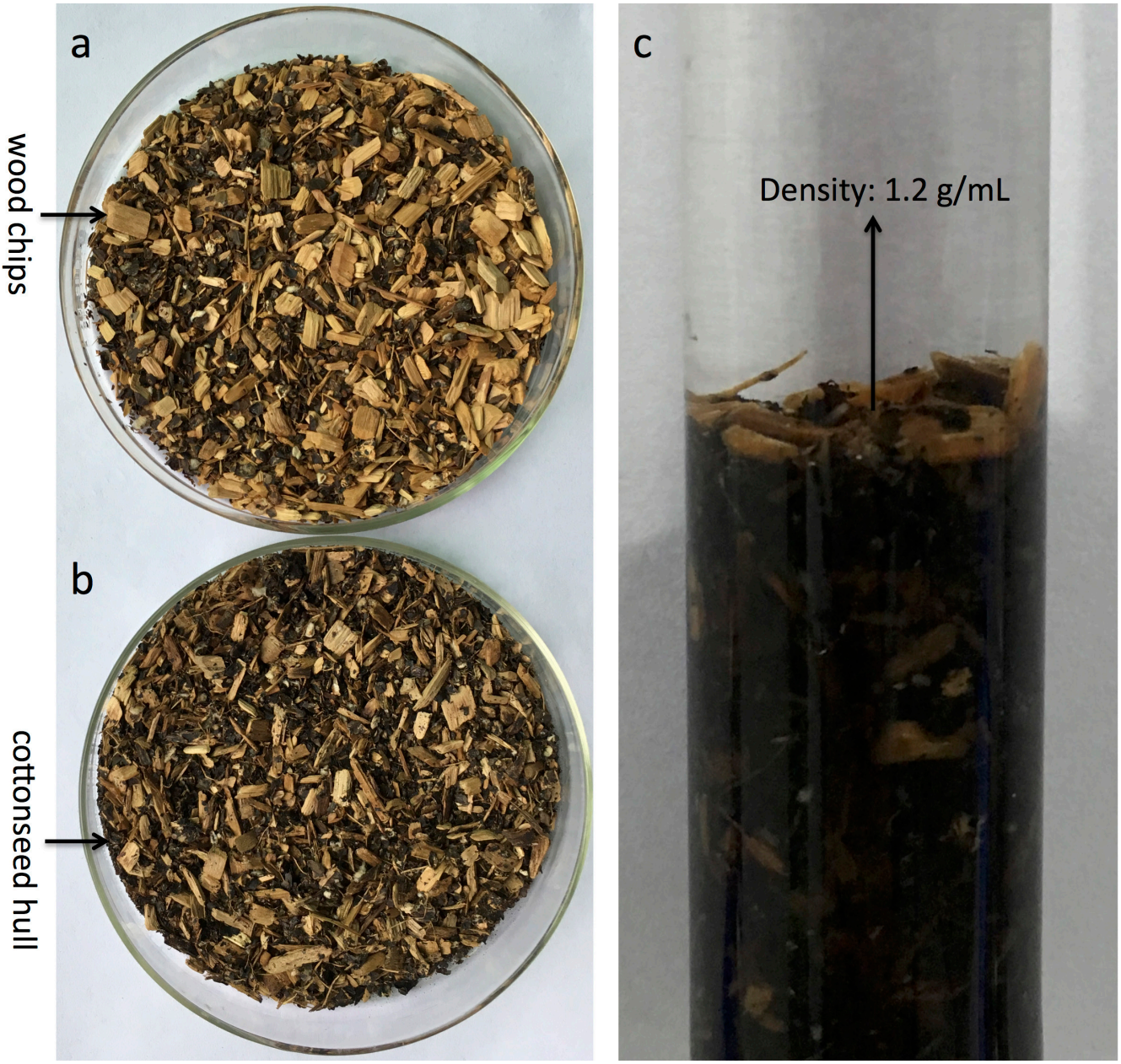

Fig. 1. Appearance of adsorbents: (a) dry SCHM, (b) dry MSCHM, (c) MSCHM in water. SCHM and MSCHM are indicative of spent compost of *Hypsizygus marmoreus* and modified spent compost of *Hypsizygus marmoreus*, respectively.

$$\ln\left(\frac{C_0}{C_t}-1\right)=\frac{K_{TH}q_0m}{Q}-K_{TH}C_0t \quad (6)$$

where K_{TH} and q_0 stands for Thomas model constant (L/min mg) and uptake capacity (mg/g), respectively, and t represents the total flow time (min). The fitted curves are shown in Fig. 3, while the detailed parameters are listed in Table 2. Undoubtedly, Thomas model was suitable for depicting the Pb(II) biosorption onto MSCHM in the fixed-bed column at operating conditions. For example, the R^2 value was 0.996, 0.993 and 0.993, and the fitted q_0 was 96.0527, 90.8629 and 83.9722 mg/g when the bed depth was 28, 20 and 12 cm, respectively.

3.5. Regeneration experiments for MSCHM

The regeneration experiments were conducted under the following conditions: 12 cm of bed depth, 30 mL/min of flow rate and 90 mg/L of Pb(II) concentration, and results are shown in Table 3. The breakthrough uptake capacity was 9.8 mg/g for cycle 1, 7.3 mg/g for cycle 2 and 5.1 mg/g for cycle 3, while the regeneration efficiency was 83% for cycle 1, 76% for cycle 2 and 73% for cycle 3. The similar tendency was seen in both breakthrough and exhaustion time since they decreased from 25 and 332 min for cycle 1 to 12 and 283 min for cycle 3, respectively. Based on these data, the parameter value decreased in cycle 3 was calculated to be 48% for the breakthrough uptake capacity, 52% for the breakthrough

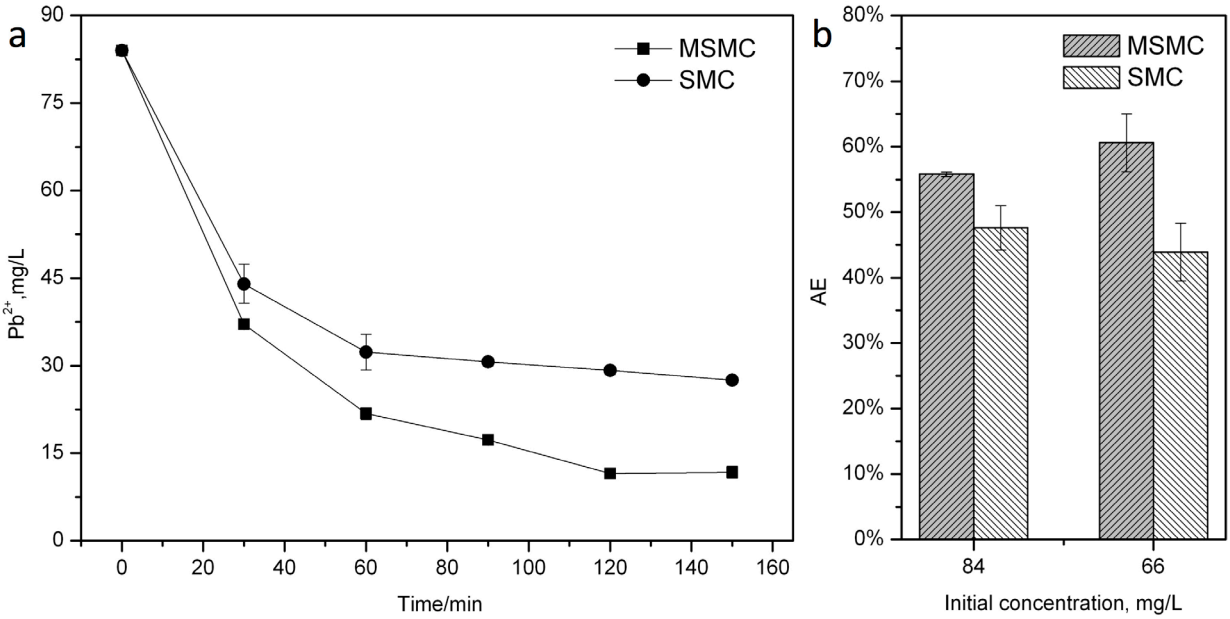

Fig. 2. Adsorption comparison between SCHM and MSCHM: (a) time course for Pb(II) adsorbed, (b) adsorption efficiency at 30 min with different initial concentration. SCHM and MSCHM are indicative of spent compost of *Hypsizygus marmoreus* and modified spent compost of *Hypsizygus marmoreus*, respectively.

Table 1
Pb(II) biosorption capacity of various composts

Composts	Sorption capacity (mg/g)	References
Sewage sludge compost	0.112	[21]
Spent mushroom compost (*Lentinus edodes*)	59.17	[22]
Household waste compost	9.79	[23]
Aquatic weed compost (*Myriophyllum spicatum*)	16.59	[24]
Eggshell-rich compost	23	[25]
Garden derived compost	4	[26]
MSCHM	72.5	This study

time, 15% for the exhaustion time and 12% for the regeneration efficiency compared with that in cycle 1.

3.6. Preliminary mechanisms for Pb(II) biosorption onto MSCHM

3.6.1. BET analysis

The textural characteristics including BET surface area and average pore diameter are listed in Table 4. The BET surface area was 1.3724 m^2/g for SCHM and 0.2732 m^2/g for MSCHM, while the average pore diameter was 8.0621 nm for SCHM and 6.5282 nm for MSCHM.

3.6.2. SEM analysis

The surface structure and morphology of SCHM and MSCHM were revealed by the scanning electron micrograph, and results are displayed in Fig. 4. It can be seen that the mycelia randomly spread on SCHM, and there were a number of cavities and debris on the external surface (Fig. 4(a)), which could help Pb^{2+} reach the interior of adsorbents easily. By comparison, as shown in Fig. 4(b), MSCHM after modification presented more irregular shape than SCHM. It seems that there were some "big cavities" on the surface of MSCHM when viewed at 1,000 magnification. However, when adsorbents were viewed at 2,000 magnification, they kept a relatively similar structure, suggesting that no obvious damage in the structure of adsorbent was caused by modification.

3.6.3. FT-IR analysis

The FT-IR technique was used to identify functional groups involved in SCHM and MSCHM. As shown in Fig. 5, several wave numbers were identified. For example, 3,344.59; 1,638.83; 1,321.21; 1,056.24 and 1,034.19 cm^{-1} were from SCHM, while 3,344.42; 1,637.33; 1,321.33; 1,056.46 and 1,034.35 cm^{-1} came from MSCHM.

4. Discussion

The removal of Pb(II) by modified spent compost of *Hypsizygus marmoreus* in a fixed-bed column was reported in this article. As mentioned above, the SMC has been used widely to removal of heavy metal ions from aqueous solution. In consideration of adsorption capability and practical feasibility, SMC was usually subject to immobilization [16,17], which would increase the treatment cost and even bring about secondary pollution. In this study, however, the spent compost of *Hypsizygus marmoreus* (SCHM) was treated simply to obtain the adsorbent with a good settling performance (Fig. 1), suggesting that MSCHM could be a fairly promising biosorbent used in engineering practice.

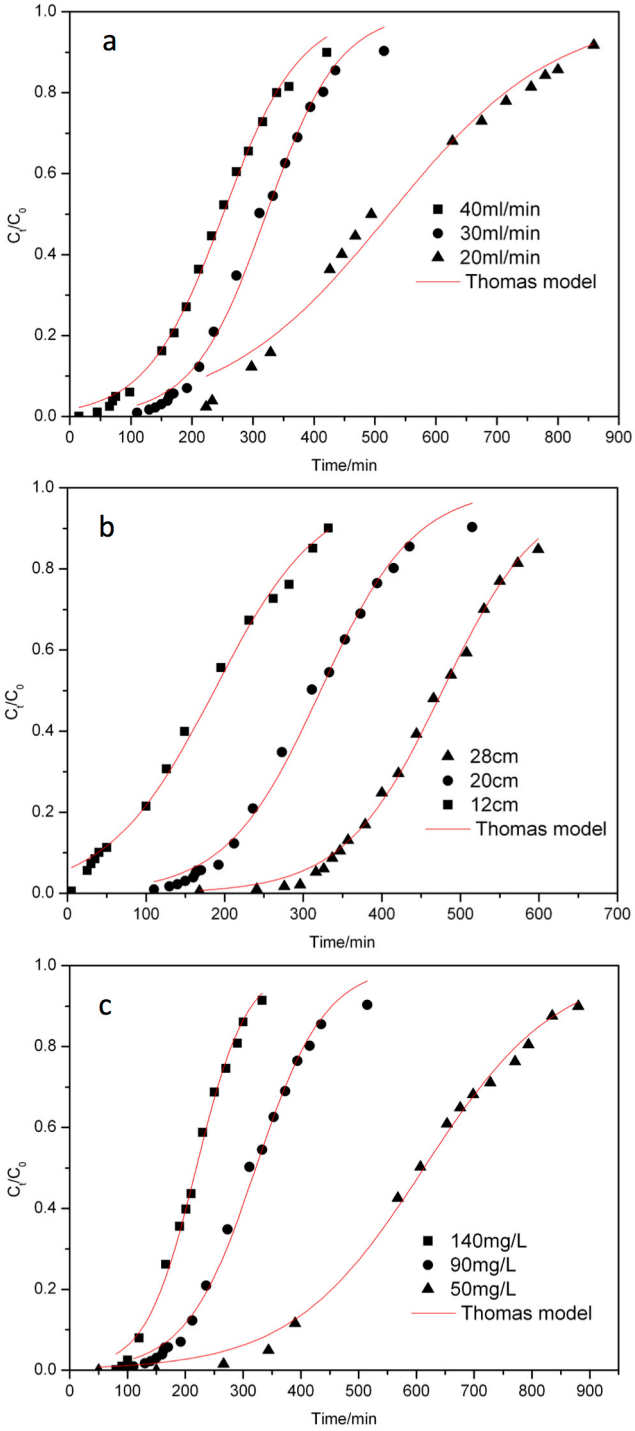

Fig. 3. Experimental and predicted breakthrough curves for Pb(II) adsorption onto MSCHM in a fixed-bed column: (a) flow rate, (b) bed depth and (c) initial concentration of Pb(II).

In batch adsorption experiments, it was found that the adsorption capacity of Pb(II) was promoted obviously after the modification of 4% NaOH solution (Fig. 2). The enhanced sorption capacity may be ascribed to the interaction with NaOH, as alkali treatment increased the H and O contents of biomass and further increased the presence of oxygen and hydrogen containing functional groups on the modified adsorbent [27]. On the other hand, NaOH can lead to the extraction of matters from the biomass, showing up new active centers in SCHM compounds in its innermost part associated with a considerable amount of metal ions adsorbed on its functional groups [28]. Accordingly, the results in batch experiments revealed that MSCHM was favorable for the Pb(II) sorption since the biosorption capacity of MSCHM was higher than that of composts as shown in Table 1.

In the fixed-bed column experiments, the effects of flow rate, bed depth and initial Pb(II) on the uptake capacity were investigated. From the results presented in Fig. 3(a), it was concluded that the flow rate had a great impact on the biosorption capability onto MSCHM. The reasons responsible for these results were (1) the fast flow rate could not leave enough time for metal ions to diffuse into the pores of sorbents thus leading to the equilibrium ahead of schedule and (2) the faster flow rate induced the less residence time, resulting in that there was no adequate time for metal ions to capture the available binding sites inside the biosorbents. The same phenomena could also be found in some reports [29,17]. On the contrary, the breakthrough and exhaustion time prolonged in proportion to the bed depth (Fig. 3(b)). These might be explained that the lower bed height reduced the diffusion of Pb(II) as the axial dispersion predominated the mass transfer, whereas the higher bed height made the metallic solution stay longer in the column to allow more metal ions to diffuse inside the biosorbent, and accommodated more biosorbents to obtain large surface area providing more active sites to bind Pb(II) ion. The relationship between the uptake capability and bed depth presented herein was in good agreement with the previous study [17]. With respect to the initial Pb(II) concentration, the uptake capacity was similar with the bed depth because of the availability of more metal ions in solution. It was reported that a higher ionic concentration would afford a higher driving force to overcome the resistances of the mass transfer from the aqueous to the solid phase [30]. However, both breakthrough and exhaustion time were shortened with the Pb(II) concentration increase (Fig. 3(c)), suggesting that higher influent concentrations caused the adsorbent to reach saturation more quickly due to the fact that lower concentration gradient would incur the deceased diffusion rate to further result in slow transport.

In this study, Thomas model was used to predict the maximum uptake capacity of MSCHM in the fixed-bed column. As listed in Table 2, the calculated q_0 values were close to the experimental q_e values, indicating the suitability of Thomas model used for column design and analysis. Meanwhile, the well-fitted data revealed that the external and internal diffusions were not the bottlenecks of the process [31]. Moreover, in order to design and optimize the fixed-bed column adsorption process, Zang et al. [17] adopted Adams–Bohart and Thomas models to predict the breakthrough curve for Cr(VI), and found that the adsorption process was better predicted and described by Thomas model, which was in conformance with the result in the current study that Thomas model was suitable for describing the Pb(II) biosorption onto MSCHM in the fixed-bed column.

It is well known that the regeneration of biosorbent is crucial for cost control in biosorption process [32], and hence the regeneration experiments were also performed in this article.

Table 2
Parameters of Thomas model

	Thomas model parameters			
	$K_{TH} \times 10^3$	q_e (mg/g)	q_0 (mg/g)	R^2
Flow rate Q (mL/min) (Bed depth 20 cm, influent concentration 90 mg/L)				
40	0.1775	87.3	90.4106	0.996
30	0.1778	87.7	90.8629	0.993
20	0.0777	97.7	98.4597	0.982
Bed depth (cm) (Flow rate 30 mL/min, influent concentration 90 mg/L)				
28	0.1698	98.7	96.0527	0.996
20	0.1778	87.7	90.8629	0.993
12	0.1644	83.2	83.9722	0.993
Influent concentration C_0 (mg/L) (Flow rate 30 mL/min, bed depth 20 cm)				
140	0.1639	94.8	92.0096	0.994
90	0.1778	87.7	90.8629	0.993
50	0.1738	83.6	82.8395	0.996

Table 3
Regeneration parameters in each cycle

Cycle no.	Breakthrough uptake capacity	Breakthrough time	Exhaustion time	Regeneration efficiency
1	9.8	25	332	83%
2	7.3	17	300	76%
3	5.1	12	283	73%

Table 4
BET characteristics of SCHM (spent compost of *Hypsizygus marmoreus*) and MSCHM (modified spent compost of *Hypsizygus marmoreus*)

	BET surface area (m^2/g)	Average pore diameter (nm)
SCHM	1.3124	8.0621
MSCHM	0.2732	6.5282

As expected, both uptake capacity and regeneration efficiency declined as sorption/desorption proceeded in the last cycle (Table 3), which was mainly attributed to the deactivation of binding sites after repeated reuse and the loss of active sites during sorption and desorption cycles. Although the regeneration efficiency dropped, it was still above 70% after three cycles, meaning that MSCHM should be a cost-effective and efficient biosorbent.

The preliminary adsorption mechanisms of Pb(II) were explored by several techniques. As shown in Table 4, the surface area and pore diameter were all decreased after NaOH modification, indicating that the modification process might exert a negative influence on BET characteristics. These phenomena were supposed to result from the fact that NaOH could lead to the extraction of matters that adhered to the biosorbent [28] and thus making the surface smooth. In spite of smaller surface area of MSCHM, its adsorption capacity could be enhanced by the increased negative charges. Besides, it has been reported that adsorption potential is inversely proportional to pore diameter, suggesting the shrunken pores might offer higher adsorption potential, which is propitious for Pb(II) adsorption [33]. Also, these results could be confirmed by SEM images (Fig. 4) where MSCHM seemed more irregular than SCHM because of modification, which made Pb(II) easily enter the interior of adsorbents. For the further mechanisms of adsorption, some functional groups were identified (Fig. 5). The wavenumbers of 3,344.59 and 3,344.42 cm^{-1} corresponded to the O–H stretch bonds of hydroxyl groups [34]. The bands at 1,638.83 and 1,637.33 cm^{-1} were attributed to N–H bending and C=O stretching in amides or the asymmetric and symmetric COO– of deprotonated carboxylate functional groups of cellulose [16]. The peaks at 1,321.21 and 1,321.33 cm^{-1} were ascribed to C–O stretching of COOH or C–N amides [35]. The wavenumbers of 1,034.19 and 1,034.35 cm^{-1} corresponded to the –OH groups (cellulosic compounds) or phosphate group in the

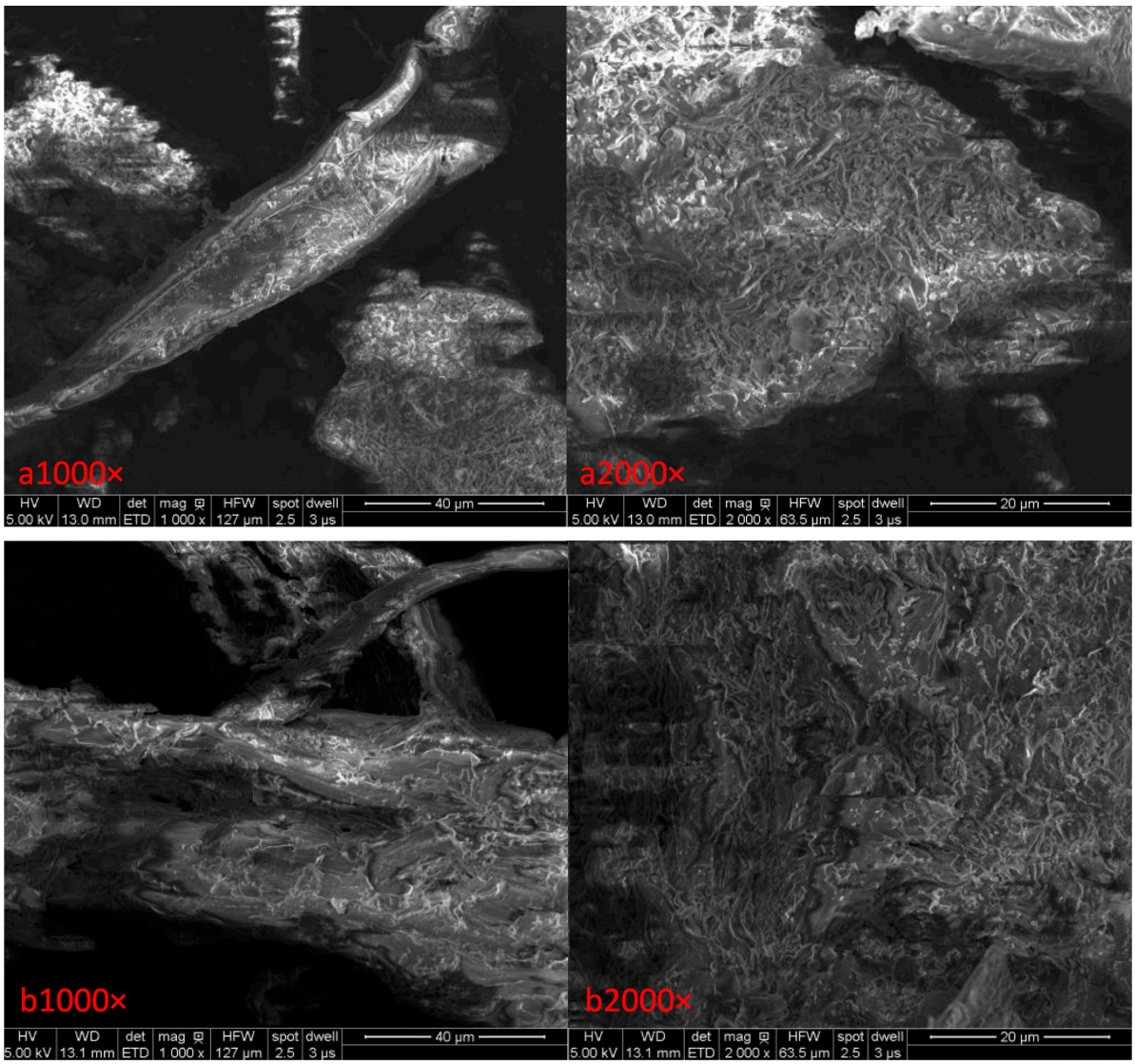

Fig. 4. SEM image of SCHM (a) and MSCHM (b). SEM represents scanning electron microscope. SCHM and MSCHM are indicative of spent compost of *Hypsizygus marmoreus* and modified spent compost of *Hypsizygus marmoreus*, respectively.

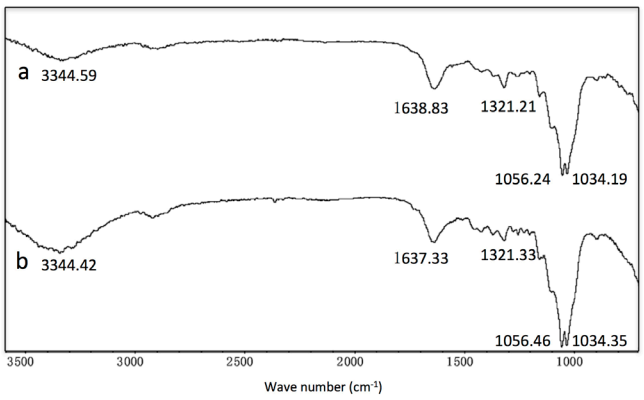

Fig. 5. FT-IR spectra for SCHM (a) and MSCHM (b). FT-IR represents Fourier transform infrared. SCHM and MSCHM are indicative of spent compost of *Hypsizygus marmoreus* and modified spent compost of *Hypsizygus marmoreus*, respectively.

biosorbent [16]. All the functional groups identified in SCHM were similar with those identified in the *Pleurotus* SMC [14]. Therefore, the functional groups of carboxyl, hydroxyl and amide may contribute to the Pb(II) ions biosorption.

5. Conclusions

The biosorption of Pb(II) using the spent compost of *Hypsizygus marmoreus* (SCHM) has been successfully carried out. The modified spent compost (MSCHM) was more propitious for Pb(II) adsorption than SCHM. The adsorption capacity in the fixed-bed column was dependent on the flow rate, bed depth and initial metal concentration and Thomas model could predict and describe the adsorption process well. The regeneration efficiency of MSCHM still maintained a relatively high level after three cycles. The preliminary adsorption mechanisms of Pb(II) were revealed by BET, SEM and FT-IR analysis. Overall, MSCHM can be a good biosorbent for cleaning wastewater containing Pb(II) ions.

Acknowledgments

This work was supported by the Significant Popularization Project of Agricultural Technology for Mushroom industry of Fujian Province (no. KNJ15301F) and the National Natural Science Foundation of China (no. 21407024). The authors would like to thank the anonymous reviewers for their promote suggestions improving the work.

References

[1] G. Corsetti, C. Romano, A. Stacchiotti, E. Pasini, F.S. Dioguardi, Endoplasmic reticulum stress and apoptosis triggered by subchronic lead exposure in mice spleen: a histopathological study, Biol. Trace Elem. Res., 178 (2017) 86–97.
[2] S. Asgary, A. Movahedian, M. Keshvari, M. Taleghani, A. Sahebkar, N. Sarrafzadegan, Serum levels of lead, mercury and cadmium in relation to coronary artery disease in the elderly: a cross-sectional study, Chemosphere, 180 (2017) 540–544.
[3] K. Conrad, H.C. Bruun Hansen, Sorption of zinc and lead on coir, Bioresour. Technol., 98 (2007) 89–97.
[4] V.K. Gupta, M. Gupta, S. Sharma, Process development for the removal of lead and chromium from aqueous solutions using red mud—an aluminium industry waste, Water Res., 35 (2001) 1125–1134.
[5] M.G. Kiran, K. Pakshirajan, G. Das, A new application of anaerobic rotating biological contactor reactor for heavy metal removal under sulfate reducing condition, Chem. Eng. J., 321 (2017) 67–75.
[6] D. Naghipour, J. Jaafari, S.D. Ashrafi, A.H. Mahvi, Remediation of heavy metals contaminated silty clay loam soil by column extraction with ethylenediaminetetraacetic acid and nitrilo triacetic acid, J. Environ. Eng., 143 (2017) 8.
[7] Z. Sekulic, D. Antanasijevic, S. Stevanovic, K. Trivunac, Application of artificial neural networks for estimating Cd, Zn, Pb removal efficiency from wastewater using complexation-microfiltration process, Int. J. Environ. Sci. Technol., 14 (2017) 1383–1396.
[8] V. Nayak, M.S. Jyothi, R.G. Balakrishna, M. Padaki, S. Deon, Novel modified poly vinyl chloride blend membranes for removal of heavy metals from mixed ion feed sample, J. Hazard. Mater., 331 (2017) 289–299.
[9] L. Wang, X.H. Zhao, J.M. Zhang, Z.H. Xiong, Selective adsorption of Pb (II) over the zinc-based MOFs in aqueous solution-kinetics, isotherms, and the ion exchange mechanism, Environ. Sci. Pollut. Res., 24 (2017) 14198–14206.
[10] P. Gikas, E. Ranieri, G. Tchobanoglous, Removal of iron, chromium and lead from waste water by horizontal subsurface flow constructed wetlands, J. Chem. Technol. Biotechnol., 88 (2013) 1906–1912.
[11] D. Sasmal, J. Maity, H. Kolya, T. Tripathy, Selective adsorption of Pb (II) ions by amylopectin-g-poly (acrylamide-co-acrylic acid): a bio-degradable graft copolymer, Int. J. Biol. Macromol., 97 (2017) 585–597.
[12] B. Ponce-Lira, E.M. Otazo-Sanchez, E. Reguera, O.A. Acevedo-Sandoval, F. Prieto-Garcia, C.A. Gonzalez-Ramirez, Lead removal from aqueous solution by basaltic scoria: adsorption equilibrium and kinetics, Int. J. Environ. Sci. Technol., 14 (2017) 1181–1196.
[13] Y. He, Q.Q. Liu, J. Hu, C.X. Zhao, C.J. Peng, Q. Yang, H.L. Wang, H.L. Liu, Efficient removal of Pb(II) by amine functionalized porous organic polymer through post-synthetic modification, Sep. Purif. Technol., 180 (2017) 142–148.
[14] A.N. Kamarudzaman, T.C. Chay, A. Amir, S.A. Talib, Biosorption of Mn(II) Ions from Aqueous Solution by Pleurotus Spent Mushroom Compost in a Fixed-bed Column, World Conference on Technology, Innovation and Entrepreneurship, 2015, pp. 2709–2716.
[15] X. Hu, L. Yan, H. Gu, T. Zang, Y. Jin, J. Qu, Biosorption mechanism of Zn^{2+} from aqueous solution by spent substrates of pleurotus ostreatus, Korean J. Chem. Eng., 31 (2014) 1911–1918.
[16] X.J. Hu, H.D. Gu, T.T. Zang, Y. Jin, J.J. Qu, Biosorption mechanism of Cu^{2+} by innovative immobilized spent substrate of fragrant mushroom biomass, Ecol. Eng., 73 (2014) 509–513.
[17] T. Zang, Z. Cheng, L. Lu, Y. Jin, X. Xu, W. Ding, J. Qu, Removal of Cr(VI) by modified and immobilized *Auricularia auricula* spent substrate in a fixed-bed column, Ecol. Eng., 99 (2017) 358–365.
[18] J.Z. Dai, F. Cen, J.H. Ji, W.W. Zhang, H. Xu, Biosorption of lead(II) in aqueous solution by spent mushroom *Tricholoma lobayense*, Water Environ. Res., 84 (2012) 291–298.
[19] S. Brunauer, P.H. Emmett, E. Teller, Adsorption of gases in multimolecular layers, J. Am. Chem. Soc., 60 (1938) 309–319.
[20] M.S. Tehrani, J.B. Ghasemi, M.T. Baharifard, Simultaneous spectrophotometric determination of zinc, cadmium and lead by xylenol orange using the partial least squares method after their preconcentration by 5,10,15,20-tetrakis(4-carboxylphenyl) porphyrin on amberlite IRA-402 resin, Asian J. Chem., 24 (2012) 3078–3086.
[21] R. Vaca, J.A. Lugo, M.V. Esteller, P. del Aguila, Soil organic matter quality and zinc and lead sorption as affected by a sewage sludge or a sewage sludge compost application, Compost Sci. Util., 16 (2008) 239–249.
[22] Y.Y. Liu, Q.Q. Zhao, G.L. Cheng, H. Xu, Exploring the mechanism of lead(II) adsorption from aqueous solution on ammonium citrate modified spent *Lentinus edodes*, Chem. Eng. J., 173 (2011) 792–800.
[23] S.M. Grimes, G.H. Taylor, J. Cooper, The availability and binding of heavy metals in compost derived from household waste, J. Chem. Technol. Biotechnol., 74 (1999) 1125–1130.
[24] J.V. Milojković, M.D. Stojanović, M.L. Mihajlović, Z.R. Lopičić, M.S. Petrović, T.D. Šoštarić, M.Đ. Ristić, Compost of aquatic weed *Myriophyllum spicatum* as low-cost biosorbent for selected heavy metal ions, Water Air Soil Pollut., 225 (2014) 1927.
[25] M.A.R. Soares, S. Marto, M.J. Quina, L. Gando-Ferreira, R. Quinta-Ferreira, Evaluation of eggshell-rich compost as biosorbent for removal of Pb (II) from aqueous solutions, Water Air Soil Pollut., 227 (2016) 150.
[26] N. Seelsaen, R. McLaughlan, S. Moore, R.M. Stuetz, Influence of compost characteristics on heavy metal sorption from synthetic stormwater, Water Sci. Technol., 55 (2007) 219–226.
[27] Z.H. Ding, X. Hu, Y.S. Wan, S.S. Wang, B. Gao, Removal of lead, copper, cadmium, zinc, and nickel from aqueous solutions by alkali-modified biochar: batch and column tests, J. Ind. Eng. Chem., 33 (2016) 239–245.
[28] J.M. Lezcano, F. Gonzalez, A. Ballester, M.L. Blazquez, J.A. Munoz, Mechanisms involved in sorption of metals by chemically treated waste biomass from irrigation pond, Environ. Earth Sci., 75 (2016) 12.
[29] V. Vinodhini, N. Das, Packed bed column studies on Cr(VI) removal from tannery wastewater by neem sawdust, Desalination, 264 (2010) 9–14.
[30] R. Sharma, B. Singh, Removal of Ni (II) ions from aqueous solutions using modified rice straw in a fixed bed column, Bioresour. Technol., 146 (2013) 519–524.
[31] W. Song, X. Xu, X. Tan, Y. Wang, J.Y. Ling, B.Y. Gao, Q.Y. Yue, Column adsorption of perchlorate by amine-crosslinked biopolymer based resin and its biological, chemical regeneration properties, Carbohydr. Polym., 115 (2015) 432–438.
[32] U. Kumar, M. Bandyopadhyay, Sorption of cadmium from aqueous solution using pretreated rice husk, Bioresour. Technol., 97 (2006) 104–109.
[33] L. Ding, A.J. Zhang, W.Q. Li, H. Bai, L. Li, Multi-length scale porous polymer films from hypercrosslinked breath figure arrays, J. Colloid Interface Sci., 461 (2016) 179–184.
[34] L. Ma, Y.H. Peng, B. Wu, D.Y. Lei, H. Xu, Pleurotus ostreatus nanoparticles as a new nano-biosorbent for removal of Mn(II) from aqueous solution, Chem. Eng. J., 225 (2013) 59–67.
[35] G. Blazquez, M.A. Martin-Lara, E. Dionisio-Ruiz, G. Tenorio, M. Calero, Copper biosorption by pine cone shell and thermal decomposition study of the exhausted biosorbent, J. Ind. Eng. Chem., 18 (2012) 1741–1750.